Nonlocal Spin Correlation as a Signature of Ising Anyons Trapped in Vacancies of the Kitaev Spin Liquid

Masahiro O. Takahashi,[1,*] Masahiko G. Yamada,[2,3,1] Masafumi Udagawa,[3]
Takeshi Mizushima,[1] and Satoshi Fujimoto[1,4]
[1]*Department of Materials Engineering Science, Osaka University, Toyonaka 560-8531, Japan*
[2]*Department of Physics, The University of Tokyo, Tokyo 113-0033, Japan*
[3]*Department of Physics, Gakushuin University, Mejiro, Toshima-ku 171-8588, Japan*
[4]*Center for Quantum Information and Quantum Biology, Osaka University, Toyonaka 560-8531, Japan*

(Received 28 November 2022; accepted 8 November 2023; published 5 December 2023)

In the Kitaev chiral spin liquid, Ising anyons are realized as Z_2 fluxes binding Majorana zero modes, which, however, are thermal excitations with finite decay rates. On the other hand, a lattice vacancy traps a Z_2 flux even in the ground state, resulting in the stable realization of a Majorana zero mode in a vacancy. We demonstrate that spin-spin correlation functions between two vacancy sites exhibit long-range correlation arising from the fractionalized character of Majorana zero modes, in spite of the strong decay of bulk spin correlations. Remarkably, this nonlocal spin correlation does not decrease as the distance between two vacancy sites increases, signaling Majorana teleportation. Furthermore, we clarify that the nonlocal correlation can be detected electrically via the measurement of nonlocal conductance between two vacancy sites, which is straightforwardly utilized for the readout of Majorana qubits. These findings pave the way to the measurement-based quantum computation with Ising anyons trapped in vacancies of the Kitaev spin liquid.

DOI: 10.1103/PhysRevLett.131.236701

Introduction.—Recent decades of the study of quantum spin liquids (QSLs) [1] unveil several properties of a new kind of matter described by topological order with fractional excitations [2]. In particular, it is extensively discussed that the fractional excitations obeying anyon statistics are utilized for the application to fault-tolerant quantum computation [3,4]. An important breakthrough in this direction was achieved by Kitaev's seminal paper on an exactly solvable spin model on a honeycomb lattice, which realizes spin liquid states with Abelian and non-Abelian anyons [5]. Subsequently, candidate materials which approximate the Kitaev model were proposed [6,7] and experimentally explored [8–14]. The low-energy properties of the Kitaev model are described by a Majorana fermion system coupled to Z_2 gauge fields, which allows for the exact analysis of the dynamics of QSLs reflecting the fractionalization of spin. Indeed, spin correlations [15–27], spin transport [28–32], and optical responses [33–35] have been studied so far, though the signature of fractionalization in physical observables is still elusive.

In the case with a magnetic field, the Kitaev model exhibits a chiral spin liquid (CSL) phase with the Chern number $\nu = \pm 1$, which hosts Ising anyons obeying non-Abelian statistics. The Ising anyon in the Kitaev spin liquid is realized as a Z_2 flux binding a Majorana zero mode (MZM), which may be detected via anyonic interferometry [36–42] or through local tunneling spectroscopy measurements in a heterostructure of Kitaev magnets and

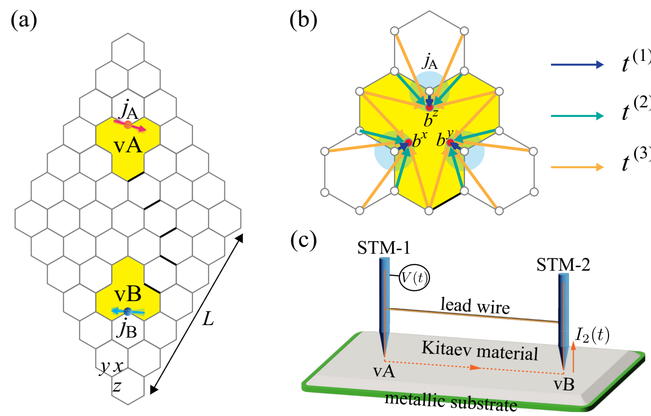

FIG. 1. (a) The Kitaev model with two vacancies, vA and vB, in the bound-flux sector. Yellow plaquettes represent the Z_2 flux. Black thick bonds denote sign-reversed Z_2 gauge fields, $u_{jk} = -1$. In our calculation, the gauge string connecting two vacancies is designed to parallel to the edge of the superlattice as shown, while no physical observable is influenced by the length or path of the gauge string, in principle, unless the flux configuration is changed. L is the system size. A periodic boundary condition is imposed. (b) The unpaired b-Majorana fermions b^x, b^y, and b^z around the vacancy vA are expressed as red circles. Hopping processes generated by a magnetic field in Eq. (2) are shown by arrows. Similar hopping processes also appear around vB. (c) A schematic setup for observing nonlocal conductance with the use of multi-STMs (see the main text for details).

conductors [43–49] or at its interface [50]. However, in the pure Kitaev model, Z_2 fluxes in the bulk are thermal excitations, and, thus, it is difficult to stabilize Ising anyons in a controllable way. One possible solution for this issue is to use site vacancies [17,27,46,51–59]. In the vicinity of a site vacancy in the Kitaev spin liquid, Z_2 fluxes emerge even in the ground state for small magnetic fields [Fig. 1(a)], so-called the bound-flux sector [51]. According to Kitaev's general argument [5], for topological phases of Majorana fermions with an odd Chern number, a MZM exists in a Z_2 flux. Thus, the vacancy in the CSL phase stabilizes MZMs in the ground state. Although the MZMs trapped in vacancies are not mobile, it is expected to perform the "braiding" of MZMs via the measurement of Majorana qubits composed of immobile MZMs [60,61], which enables measurement-based quantum computation.

In this Letter, we investigate the scheme for the simultaneous detection and the manipulation of Ising anyons trapped in spatially well-separated vacancies of the Kitaev spin liquid. Our main idea is to explore for nonlocal correlation (or teleportation) of MZMs [62–66] trapped in vacancies. Teleportation mediated via MZMs was originally proposed by Fu [62] in the case of topological superconductors. For realizing Majorana teleportation, the parity of the total fermion number must be conserved. The crucial idea of Ref. [62] is to use a mesoscopic superconductor with charging energy for preserving the fermion parity. However, this idea is not applicable to the case of a Kitaev material which is a Mott insulator. Instead, we exploit a quite different idea based on Mottness; for the Kitaev spin liquid, the system allows only single-electron occupation per one site, and, thus, fermion parity conservation is strictly realized. We demonstrate that teleportation of the MZMs trapped in vacancies is observable in spin correlation functions; i.e., it exhibits long-range correlation in the spin-gapped phase, in spite of the strong decay of bulk spin correlation. Since spin correlation functions of the Kitaev spin liquid are expressed in terms of correlations of Majorana fields, Majorana teleportation naturally leads to the long-range spin correlation. Furthermore, the nonlocal correlation can be detected electrically via the measurement of the nonlocal conductance for a thin film of the Kitaev material placed on a metallic substrate. This scheme straightforwardly allows the measurement-based braiding of Ising anyons trapped in vacancies and their application to topological quantum computation.

Effective Hamiltonian.—We consider the Kitaev model on $L \times L$ unit cells system with two vacancies, vA and vB [Fig. 1(a)], under a magnetic field $\boldsymbol{h} = (h_x, h_y, h_z)$. The Hamiltonian is

$$H = -J \sum_{\substack{cj,k \neq \mathrm{vA,vB} \\ \langle jk \rangle_\gamma}} S_j^\gamma S_k^\gamma - h_\gamma \sum_{j \neq \mathrm{vA,vB}} S_j^\gamma, \tag{1}$$

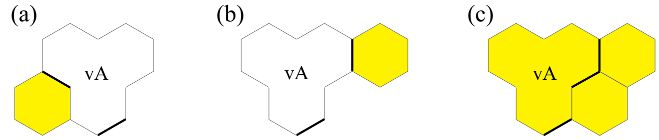

FIG. 2. (a)–(c) Z_2 flux excitations around a vacancy with the energy cost Δ_{in}, Δ_{out}, and Δ_{tri}, respectively.

where $\langle jk \rangle_\gamma$ denotes nearest-neighbor (NN) sites j and k connected by a $\gamma (= x, y, z)$ bond, S_j^γ is the γ component of an $s = 1/2$ spin operator on a site j, and J represents the strength of the Kitaev interaction. The second term is the Zeeman interaction that drives the system into the CSL phase. For concreteness, we fix the direction of $\boldsymbol{h}$ parallel to the in-plane crystallographic a axis $(1, 1, \bar{2})$, though our main results are qualitatively not affected by the field direction unless the field-induced Majorana gap is closed. In the Kitaev spin liquid state, the spin operator is decomposed into two Majorana fields as $S_j^\gamma = (i/2) b_j^\gamma c_j$, where c_j is an itinerant Majorana field and b_j^γ is a localized gauge Majorana field. In the pure Kitaev model, every b-Majorana field is paired with a nearest-neighbor b-Majorana field, constituting a Z_2 gauge field $u_{jk}^\gamma = i b_j^\gamma b_k^\gamma$ on a γ bond connecting the sites j and k. However, in the case with vacancies, there are three unpaired b-Majorana fields around a vacancy as shown in Fig. 1(b). These unpaired b-Majorana fermions are coupled to itinerant c-Majorana fermions via a magnetic field. Furthermore, for a weak magnetic field, a Z_2 flux is stably trapped in a vacancy even in the ground state [51]. Note that there are three patterns of the changes of Z_2 flux configurations around a vacancy as shown in Figs. 2(a)–2(c). The excitation energies from the bound-flux sector to these three sectors are $\Delta_{\mathrm{in}} \approx 0.055J$, $\Delta_{\mathrm{out}} \approx 0.035J$, and $\Delta_{\mathrm{tri}} \approx 0.058J$, respectively [67]. Taking account of these points and treating the magnetic field perturbatively, we construct the effective Majorana Hamiltonian for the bound-flux sector of the CSL phase:

$$H_{\mathrm{eff}} = \frac{1}{4}\left(H_{\mathrm{NN}} + H_{\mathrm{NNN}} + \sum_{i=1,2,3} H_{b\text{-Majo}}^{(i)} \right), \tag{2}$$

where the normalization factor $1/4$ is chosen, since the Lie algebra of $-iH_{\mathrm{eff}}$ is identified with $so(2L^2 + 4)$. H_{NN} contains the NN hopping of itinerant Majorana fermions coupled with a Z_2 gauge field on a γ bond u_{jk}^γ. H_{NNN} is the next-nearest-neighbor (NNN) hopping term, which generates the energy gap of itinerant Majorana fermions. The other three terms, $H_{b\text{-Majo}}^{(i)}$ $(i = 1, 2, 3)$, express hopping processes between itinerant Majorana fermions and the unpaired b-Majorana fermions adjacent to each vacancy [see Fig. 1(b)]. Every hopping amplitude depends on its location, since the energy cost of changing a flux

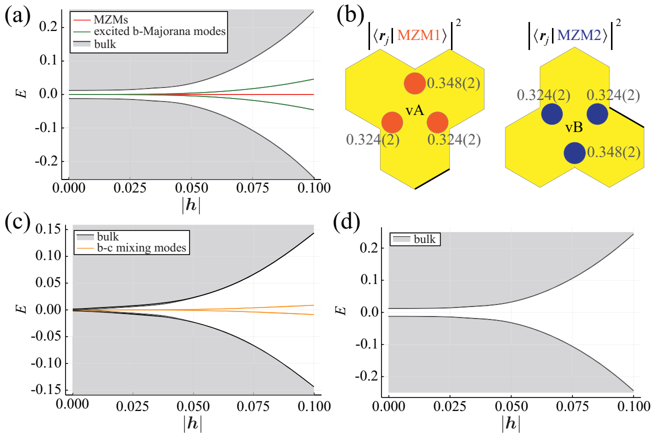

FIG. 3. (a) The energy spectrum versus $|\boldsymbol{h}|$ for the bound-flux sector for the $L = 80$ system. (b) Spatial distribution of the squared probability amplitudes of MZMs around vacancies vA and vB. (c) The energy spectrum versus $|\boldsymbol{h}|$ for the zero-flux sector. (d) The energy spectrum versus $|\boldsymbol{h}|$ for the bound-flux sector without the coupling with the unpaired b-Majorana fermions.

configuration is different around vacancies, and this point is explained precisely in Supplemental Material [67].

Majorana zero modes trapped in vacancies.—For a weak magnetic field, $0 \leq |\boldsymbol{h}| \leq 0.15$, the bound-flux sector is the ground state of H_{eff}, as was pointed out by previous studies [51,57]. Here, we explore for MZMs in Z_2 fluxes trapped in vacancies. The energy spectrum of Majorana fermions as functions of a magnetic field is shown in Fig. 3(a). At $|\boldsymbol{h}| = 0.0$, in addition to the bulk energy continuum, there are six localized zero modes, which is obvious, since six b-Majorana fermions neighboring the two vacancies are uncoupled with itinerant Majorana fermions. For a nonzero magnetic field, on the other hand, they split into two sets of distinct states; one is a pair of zero-energy states, $|\mathrm{MZM}+\rangle$ and $|\mathrm{MZM}-\rangle$, which are colored red, and the other are two particle-hole pairs of excited b-Majorana modes, colored green. The MZMs are located adjacent to the vacancies as seen in Fig. 3(b). In this figure, the squared probability amplitudes of $|\mathrm{MZM}1,2\rangle \equiv (|\mathrm{MZM}+\rangle \mp |\mathrm{MZM}-\rangle)/\sqrt{2}$ at each site are shown, and, for $|\boldsymbol{h}| = 0.05$, 99.6(6)% of them are on the sites neighboring vA or vB, where there are b-Majorana fermions which are not paired into gauge fields. The relative weight of the probability amplitude at each site, $|\langle \boldsymbol{r}_j|\mathrm{MZM}1,2\rangle|^2$, depends on the direction of an external field. We emphasize that, for the realization of the MZMs shown in Fig. 3(a), the hopping processes between unpaired b-Majorana fermions and itinerant c-Majorana fermions, described by $H^{(i)}_{b\text{-Majo}}$, in the bound-flux sector are crucially important. In fact, if one neglect these contributions, no stable MZMs appear as shown in Figs. 3(c) and 3(d). In the case of the zero-flux sector, for instance, the low-energy states in the Majorana gap, as shown in Fig. 3(c), are mixing modes composed of c-Majorana fermions and unpaired b-Majorana fermions adjacent to the vacancies, which is distinguishable from MZMs. Besides, it is worth mentioning that the Majorana bulk gap structure at zero magnetic fields in the finite system strongly depends on the local Z_2 gauge fields. In fact, for the bound-flux sector, the system acquires the bulk gap as in Figs. 3(a) and 3(d).

Nonlocal correlation due to MZMs.—One of the distinct features of Majorana particles is nonlocal correlation or teleportation arising from the fractionalized character. We, here, demonstrate that nonlocal correlation of MZMs trapped in vacancies of the CSL phase can appear in magnetic responses. We consider the nonlocal spin correlation function between two sites adjacent to vacancies as depicted in Fig. 1(a):

$$\langle S^z_{j_A}(t) S^z_{j_B}(0)\rangle \equiv \frac{\mathrm{Tr}[P_F S^z_{j_A}(t) S^z_{j_B}(0) e^{-\beta H_{\mathrm{eff}}}]}{\mathrm{Tr}[P_F e^{-\beta H_{\mathrm{eff}}}]}. \quad (3)$$

Here, P_F is a projection operator to the physical subspace satisfying $\prod_j D_j = 1$ with $D_j = b^x_j b^y_j b^z_j c_j$ [5,68]. In the zero-flux sector of the pure Kitaev model, only the spin-spin correlation between the NN sites is nonzero, and any other spin-spin correlations vanish, characterizing the spin liquid state. On the other hand, the nonlocal correlation mediated by spatially well-separated MZMs leads to long-range spin correlation as we see below. Note that the spin correlation considered here is quite different from that discussed in Ref. [16], where the bulk spin correlation induced by a magnetic field was considered. Utilizing a technique developed before by one of the authors [55], we obtain the formula of the dynamical spin correlation function [67]. The results for the equal-time correlation $\langle S^z_{j_A}(0) S^z_{j_B}(0)\rangle$ calculated for a $L = 40$ system are summarized in Fig. 4(a). Here, the trivial contributions from the magnetization induced by a magnetic field are extracted to focus on nonlocal correlation. It is clearly seen that, for the weak field region corresponding to the bound-flux sector, prominent nonlocal correlations appear. Also, the correlations do not decrease exponentially as the distance between the two vacancies increases, as shown in Fig. 4(b). Actually, the origin of the nonlocal correlations shall not be described by the overlap between two wave functions of MZMs trapped in each vacancy, since their spatial decay rates are fast enough as in Fig. 3(b), and one needs an alternative picture. These results imply that the long-range spin correlations are mediated by teleportation of MZMs located around the vacancies.

To confirm that the nonlocal correlations arise from MZMs, we computed the Fourier transformation of the time-dependent spin correlation function defined as

$$\Psi^{zz}_{j_A,j_B}(\omega + i\delta) = \int_0^\infty dt e^{i(\omega+i\delta)t} \langle S^z_{j_A}(t) S^z_{j_B}(0)\rangle, \quad (4)$$

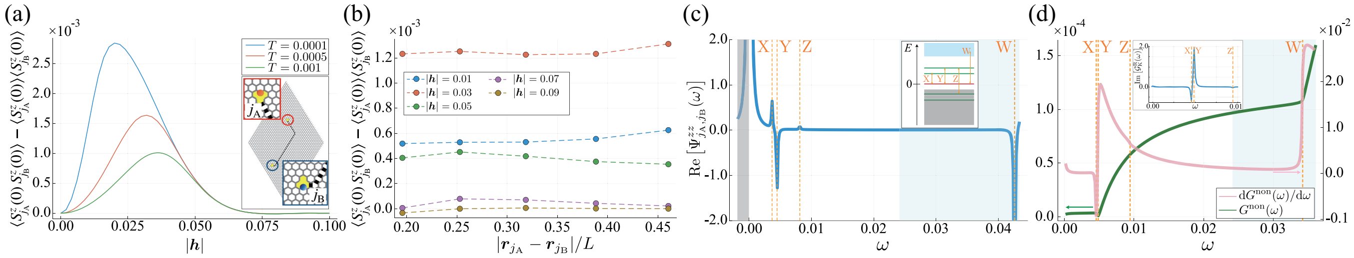

FIG. 4. (a) The equal-time nonlocal spin correlations versus $|\boldsymbol{h}|$ at several temperatures. The inset shows the $L = 40$ system with two vacancies spatially well separated. (b) The equal-time nonlocal spin correlations versus the distance between the two vacancies for several values of $|\boldsymbol{h}|$. (c) The ω dependence of the real part of the dynamical spin correlation function for the $L = 40$ system with $|\boldsymbol{h}| = 0.05$. The frequencies corresponding to energy levels of Majorana bound states near vacancies are indicated by orange vertical lines. The gray region represents energies below the chemical potential, and the blue region corresponds for the bulk continuum above the bulk energy gap. The inset shows Majorana spectrums including MZMs and excited b-Majorana modes near vacancies. (d) The nonlocal conductance and its ω derivative calculated for the $L = 24$ system with $|\boldsymbol{h}| = 0.05$. The vertical axis of conductance is normalized by the conductance of the lead wire, and we set the tunneling amplitude t_1 equal to the magnitude of the Kitaev interaction. The inset shows the imaginary part of the retarded nonlocal spin-spin correlation for the low-frequency region.

with $\delta \ll 1$. The numerical results are shown in Fig. 4(c). Around $\omega = 0$, the Dirac-delta-function-like peak appears from the time-independent part of $\Psi^{zz}_{j_A,j_B}$ which is due to local magnetizations induced by a magnetic field. On the other hand, there are two peaks and one dip structure inside the itinerant Majorana bulk gap that signify the existence of MZMs and excited b-Majorana modes in the vacancies. In fact, we see that the frequencies associated with these structures exactly coincide with excitation energies labeled by X, Y, and Z in the inset in Fig. 4(c). Since the ω dependence of the dynamical spin correlation function is determined by two-fermion excitation processes, the characteristic energy scale is $E_b - E_{\mathrm{MZM}}$, where E_b is the energy level of an excited b-Majorana mode and E_{MZM} is that of a MZM. The low-energy structures of $\Psi^{zz}_{j_A,j_B}(\omega)$ reflect these energy scales. Thus, we can conclude that the long-range spin correlation between two vacancies arises from MZMs trapped in the vacancies. In other words, it arises from teleportation of MZMs [62]. That is, since $\Psi^{zz}_{j_A,j_B}(E_b - E_{\mathrm{MZM}}) \propto \langle i\gamma_A\gamma_B\rangle$, where $\gamma_{A(B)}$ is the Majorana field for the zero mode near the vacancy vA (vB), the conservation of fermion parity $\langle i\gamma_A\gamma_B\rangle \neq 0$ leads to long-range correlation. In the case of topological superconductors, for preserving the fermion parity necessary for Majorana teleportation, the charging energy must be imposed [62]. On the other hand, for the Kitaev spin liquid, the fermion parity conservation is intrinsically ensured by the Mott physics. Although, we, here, concentrate on the z component of the spin correlation, similar behaviors appear also in other spin components.

Nonlocal conductance and the measurement-based manipulation of MZMs.—We, here, reveal that the nonlocal spin correlation due to vacancy-trapped Ising anyons can be electrically detected via the measurement of nonlocal conductance whose ω dependence captures the feature of MZMs. A schematic setup we propose is shown in Fig. 1(c): Two STM tips are located on top of each vacancy, vA and vB, of the Kitaev material monolayer upon a metal substrate, and an ac voltage with the frequency $\omega > 0$, $V(t) = V_1 e^{-i\omega t}$, is applied to one of the STM tips, say, STM-1. A lead connecting the two STM tips is optionally introduced to realize nonvanishing electric correlation between the tips. It is noted that the Kitaev monolayer on a metal substrate such as graphene can be fabricated by currently available techniques for van der Waals heterostructure systems [43,69–73]. Assuming the exchange interaction between spins of the Kitaev material and electron spins in the tips and the substrate [43] and using the Kubo formula, we obtain the time-dependent electric current at STM-2, $I_2(t)$. Then, the nonlocal conductance is given by [67]

$$G^{\mathrm{non}}(\omega) \equiv \frac{\mathrm{d}I_2(\omega)}{\mathrm{d}V_1} \propto 2e^2 \frac{\mathrm{Im}\mathcal{K}^R(\omega)}{\omega}, \tag{5}$$

$$\mathrm{Im}\mathcal{K}^R(\omega) \sim \int_{-\omega}^{0} \frac{d\omega'}{2\pi} C\omega' \mathrm{Im}\mathcal{G}^R_K(\omega' + \omega). \tag{6}$$

Here, C is a constant proportional to t_1^2 with t_1 a spin-dependent tunneling amplitude, and $\mathcal{G}^R_K(\omega')$ is the Fourier transform of a retarded nonlocal spin correlation function of the Kitaev material, $\mathcal{G}^R_K(t - t') \equiv -i\theta(t - t')\langle[S^z_{j_A}(t), S^z_{j_B}(t')]\rangle$. Although, in general, all the components of the spin correlation functions, $\langle S^\alpha_A S^\beta_B\rangle$, contribute to the conductance, their ω dependence, which is important for the detection of MZMs, is qualitatively similar. Thus, for simplicity, we here consider only the z-z component of nonlocal spin correlations. The ω dependence of $G^{\mathrm{non}}(\omega)$ clearly signifies the existence of MZMs as seen in Fig. 4(d). The kink and dip structures at X and Y, respectively, in Fig. 4(d) correspond to the peak structures of the spin correlation function associated with MZMs shown in the inset in Fig. 4(d). Note that, since the nonlocal conductance is proportional to t_1^2, its magnitude can be enhanced by an order of magnitude if larger t_1 is used. Thus, the signature of MZMs can be clearly detected in the low-frequency structure of $G^{\mathrm{non}}(\omega)$. This result is also utilized for the readout of Majorana qubits, since, as mentioned before, the nonlocal spin correlation is proportional to the eigenvalue of the Majorana qubit $i\gamma_A\gamma_B$. Furthermore, this makes it possible to use Ising anyons trapped in vacancies for the measurement-based quantum computation [60,61].

Discussion.—We briefly discuss the effect of the non-Kitaev interactions on nonlocal correlations. According to Ref. [74], off-diagonal interactions called Γ and Γ' terms enhance the Majorana bulk gap within a perturbative treatment. Thus, as long as the Kitaev spin liquid state is realized, the non-Kitaev interactions have the potential to stabilize the nonlocal spin correlation. Indeed, we have carried out some calculations in the system with Γ' term and confirm that the peak of the equal-time nonlocal spin correlations is slightly increased by the enhancement of the bulk gap [67].

Summary.—It has been clarified that the signature of Ising anyons trapped in vacancies of the Kitaev spin liquid appears in nonlocal spin correlations between two vacancy sites, which exhibit long-range correlation arising from the teleportation of MZMs. We have also proposed the scheme for detecting the nonlocal correlation via the measurement of nonlocal conductance, which implies the application to the readout and manipulation of Majorana qubits for quantum computation.

We thank Y. Matsuda, T. Shibauchi, Y. Kasahara, K. Hashimoto, T. Asaba, and S. Suetsugu for fruitful discussions. M. O. T. is supported by a Japan Society for the Promotion of Science (JSPS) Fellowship for Young Scientists and by Program for Leading Graduate Schools: "Interactive Materials Science Cadet Program." M. G. Y. is supported by Multidisciplinary Research Laboratory System for Future Developments, Osaka University, and Japan Science and Technology Agency (JST) Grant No. JPMJPR225B, as well as the Center of Innovations for Sustainable Quantum AI (JST Grant No. JPMJPF2221). This work was supported by JST CREST Grant No. JPMJCR19T5, Japan, and the Grants-in-Aid for Scientific Research on Innovative Areas "Quantum Liquid Crystals (No. JP22H04480)" from JSPS of Japan, and JSPS KAKENHI (Grants No. JP20K03860, No. JP20H01857, No. JP20H05655, No. JP21H01039, No. JP22K14005, No. JP22H01147, No. JP22H01221, and No. JP22J20066).

*takahashi@blade.mp.es.osaka-u.ac.jp

[1] C. Broholm, R. J. Cava, S. A. Kivelson, D. G. Nocera, M. R. Norman, and T. Senthil, Science **367**, eaay0668 (2020).
[2] X.-G. Wen, Phys. Rev. B **65**, 165113 (2002).
[3] A. Kitaev, Ann. Phys. (Amsterdam) **303**, 2 (2003).
[4] C. Nayak, S. H. Simon, A. Stern, M. Freedman, and S. Das Sarma, Rev. Mod. Phys. **80**, 1083 (2008).
[5] A. Kitaev, Ann. Phys. (Amsterdam) **321**, 2 (2006), January Special Issue.
[6] G. Jackeli and G. Khaliullin, Phys. Rev. Lett. **102**, 017205 (2009).
[7] J. c. v. Chaloupka, G. Jackeli, and G. Khaliullin, Phys. Rev. Lett. **105**, 027204 (2010).
[8] L. J. Sandilands, Y. Tian, K. W. Plumb, Y.-J. Kim, and K. S. Burch, Phys. Rev. Lett. **114**, 147201 (2015).
[9] A. Banerjee, C. A. Bridges, J.-Q. Yan, A. A. Aczel, L. Li, M. B. Stone, G. E. Granroth, M. D. Lumsden, Y. Yiu, J. Knolle, S. Bhattacharjee, D. L. Kovrizhin, R. Moessner, D. A. Tennant, D. G. Mandrus, and S. E. Nagler, Nature (London) **15**, 733 (2016).
[10] S.-H. Baek, S.-H. Do, K.-Y. Choi, Y. S. Kwon, A. U. B. Wolter, S. Nishimoto, J. van den Brink, and B. Büchner, Phys. Rev. Lett. **119**, 037201 (2017).
[11] S.-H. Do, S.-Y. Park, J. Yoshitake, J. Nasu, Y. Motome, Y. S. Kwon, D. T. Adroja, D. J. Voneshen, K. Kim, T. H. Jang, J. H. Park, K.-Y. Choi, and S. Ji, Nat. Phys. **13**, 1079 (2017).
[12] N. Jansa, A. Zorko, M. Gomilsek, M. Pregeli, K. W. Krämer, D. Biner, A. Biffin, C. Rüegg, and M. Klanjsek, Nat. Phys. **14**, 786 (2018).
[13] Y. Kasahara, T. Ohnishi, Y. Mizukami, O. Tanaka, S. Ma, K. Sugii, N. Kurita, H. Tanaka, J. Nasu, Y. Motome, T. Shibauchi, and Y. Matsuda, Nature (London) **559**, 227 (2018).
[14] O. Tanaka, Y. Mizukami, R. Harasawa, K. Hashimoto, K. Hwang, N. Kurita, H. Tanaka, S. Fujimoto, Y. Matsuda, E. G. Moon, and T. Shibauchi, Nat. Phys. **18**, 429 (2022).
[15] G. Baskaran, S. Mandal, and R. Shankar, Phys. Rev. Lett. **98**, 247201 (2007).
[16] K. S. Tikhonov, M. V. Feigel'man, and A. Y. Kitaev, Phys. Rev. Lett. **106**, 067203 (2011).
[17] F. Trousselet, G. Khaliullin, and P. Horsch, Phys. Rev. B **84**, 054409 (2011).
[18] S. R. Hassan, P. V. Sriluckshmy, S. K. Goyal, R. Shankar, and D. Sénéchal, Phys. Rev. Lett. **110**, 037201 (2013).
[19] J. Knolle, D. L. Kovrizhin, J. T. Chalker, and R. Moessner, Phys. Rev. Lett. **112**, 207203 (2014).
[20] J. Knolle, D. L. Kovrizhin, J. T. Chalker, and R. Moessner, Phys. Rev. B **92**, 115127 (2015).
[21] X.-Y. Song, Y.-Z. You, and L. Balents, Phys. Rev. Lett. **117**, 037209 (2016).
[22] D. Gotfryd, J. Rusnačko, K. Wohlfeld, G. Jackeli, J. c. v. Chaloupka, and A. M. Oleś, Phys. Rev. B **95**, 024426 (2017).
[23] S. Liang, B.-S. He, Z.-Y. Dong, W. Chen, J.-X. Li, and Q.-H. Wang, Phys. Rev. B **98**, 104410 (2018).
[24] D. Otten, A. Roy, and F. Hassler, Phys. Rev. B **99**, 035137 (2019).
[25] A. Lunkin, K. Tikhonov, and M. Feigel'man, J. Phys. Chem. Solids **128**, 130 (2019).
[26] W. Choi, K. H. Lee, and Y. B. Kim, Phys. Rev. Lett. **124**, 117205 (2020).
[27] J. Nasu and Y. Motome, Phys. Rev. B **104**, 035116 (2021).

[28] T. Minakawa, Y. Murakami, A. Koga, and J. Nasu, Phys. Rev. Lett. **125**, 047204 (2020).
[29] H. Taguchi, Y. Murakami, A. Koga, and J. Nasu, Phys. Rev. B **104**, 125139 (2021).
[30] H. Taguchi, Y. Murakami, and A. Koga, Phys. Rev. B **105**, 125137 (2022).
[31] J. Nasu, Y. Murakami, and A. Koga, Phys. Rev. B **106**, 024411 (2022).
[32] D. Takikawa, M. G. Yamada, and S. Fujimoto, Phys. Rev. B **105**, 115137 (2022).
[33] J. Knolle, G.-W. Chern, D. L. Kovrizhin, R. Moessner, and N. B. Perkins, Phys. Rev. Lett. **113**, 187201 (2014).
[34] J. Nasu, J. Knolle, D. L. Kovrizhin, Y. Motome, and R. Moessner, Nat. Phys. **12**, 912 (2016).
[35] M. Kanega, T. N. Ikeda, and M. Sato, Phys. Rev. Res. **3**, L032024 (2021).
[36] D. Aasen, R. S. K. Mong, B. M. Hunt, D. Mandrus, and J. Alicea, Phys. Rev. X **10**, 031014 (2020).
[37] K. Klocke, D. Aasen, R. S. K. Mong, E. A. Demler, and J. Alicea, Phys. Rev. Lett. **126**, 177204 (2021).
[38] Z. Wei, V. F. Mitrović, and D. E. Feldman, Phys. Rev. Lett. **127**, 167204 (2021).
[39] K. Klocke, J. E. Moore, J. Alicea, and G. B. Halász, Phys. Rev. X **12**, 011034 (2022).
[40] Y. Liu, K. Slagle, K. S. Burch, and J. Alicea, Phys. Rev. Lett. **129**, 037201 (2022).
[41] Z. Wei, N. Batra, V. F. Mitrović, and D. E. Feldman, Phys. Rev. B **107**, 104406 (2023).
[42] G. B. Halász, arXiv:2308.05154.
[43] J. Feldmeier, W. Natori, M. Knap, and J. Knolle, Phys. Rev. B **102**, 134423 (2020).
[44] R. G. Pereira and R. Egger, Phys. Rev. Lett. **125**, 227202 (2020).
[45] E. J. König, M. T. Randeria, and B. Jäck, Phys. Rev. Lett. **125**, 267206 (2020).
[46] M. Udagawa, S. Takayoshi, and T. Oka, Phys. Rev. Lett. **126**, 127201 (2021).
[47] T. Bauer, L. R. D. Freitas, R. G. Pereira, and R. Egger, Phys. Rev. B **107**, 054432 (2023).
[48] W.-H. Kao, N. B. Perkins, and G. B. Halász, arXiv:2307.10376.
[49] W.-H. Kao, G. B. Halász, and N. B. Perkins, arXiv:2310.06891.
[50] G. Kishony and E. Berg, Phys. Rev. B **104**, 235118 (2021).
[51] A. J. Willans, J. T. Chalker, and R. Moessner, Phys. Rev. Lett. **104**, 237203 (2010).
[52] A. J. Willans, J. T. Chalker, and R. Moessner, Phys. Rev. B **84**, 115146 (2011).
[53] S. G., V. Sreenath, A. Lakshminarayan, and R. Narayanan, Phys. Rev. B **85**, 054204 (2012).
[54] G. B. Halász, J. T. Chalker, and R. Moessner, Phys. Rev. B **90**, 035145 (2014).
[55] M. Udagawa, Phys. Rev. B **98**, 220404(R) (2018).
[56] J. Nasu and Y. Motome, Phys. Rev. B **102**, 054437 (2020).
[57] W.-H. Kao, J. Knolle, G. B. Halász, R. Moessner, and N. B. Perkins, Phys. Rev. X **11**, 011034 (2021).
[58] W.-H. Kao and N. B. Perkins, Ann. Phys. (Amsterdam) **435**, 168506 (2021), special issue on Philip W. Anderson.
[59] V. Dantas and E. C. Andrade, Phys. Rev. Lett. **129**, 037204 (2022).
[60] P. Bonderson, M. Freedman, and C. Nayak, Phys. Rev. Lett. **101**, 010501 (2008).
[61] S. Vijay and L. Fu, Phys. Rev. B **94**, 235446 (2016).
[62] L. Fu, Phys. Rev. Lett. **104**, 056402 (2010).
[63] A. Zazunov, A. L. Yeyati, and R. Egger, Phys. Rev. B **84**, 165440 (2011).
[64] R. Hützen, A. Zazunov, B. Braunecker, A. L. Yeyati, and R. Egger, Phys. Rev. Lett. **109**, 166403 (2012).
[65] M. Sato and S. Fujimoto, J. Phys. Soc. Jpn. **85**, 072001 (2016).
[66] J. Reslen, J. Phys. Commun. **2**, 105006 (2018).
[67] See Supplemental Material at http://link.aps.org/supplemental/10.1103/PhysRevLett.131.236701 for more details.
[68] F. L. Pedrocchi, S. Chesi, and D. Loss, Phys. Rev. B **84**, 165414 (2011).
[69] B. Zhou, J. Balgley, P. Lampen-Kelley, J.-Q. Yan, D. G. Mandrus, and E. A. Henriksen, Phys. Rev. B **100**, 165426 (2019).
[70] M. Carrega, I. J. Vera-Marun, and A. Principi, Phys. Rev. B **102**, 085412 (2020).
[71] E. Gerber, Y. Yao, T. A. Arias, and E.-A. Kim, Phys. Rev. Lett. **124**, 106804 (2020).
[72] H.-K. Jin and J. Knolle, Phys. Rev. B **104**, 045140 (2021).
[73] Z. Wang, L. Liu, H. Zheng, M. Zhao, K. Yang, C. Wang, F. Yang, H. Wu, and C. Gao, Nanoscale **14**, 11745 (2022).
[74] D. Takikawa and S. Fujimoto, Phys. Rev. B **99**, 224409 (2019).